Supplementary Information

The two-dimensional *n/p* type carriers at the interface of $LaAlO_3/KTaO_3$ heterostructures

Yirong Geng[1], Zuhui Hu[1], Chang Liu[1], Ruiling Gao[1], Hui Zhang[1], Le Fang[2*], Wei Ren[1*]

[1] *Physics Department, Materials Genome Institute, Shanghai Engineering Research Center for Integrated Circuits and Advanced Display Materials, Institute for Quantum Science and Technology, International Centre of Quantum and Molecular Structures, Shanghai University, Shanghai 200444, China*

[2] *School of Materials, Shanghai Dianji University, Shanghai 201306, China*

renwei@shu.edu.cn; fangle@sdju.edu.cn; changliu@shu.edu.cn; hzhang23@shu.edu.cn

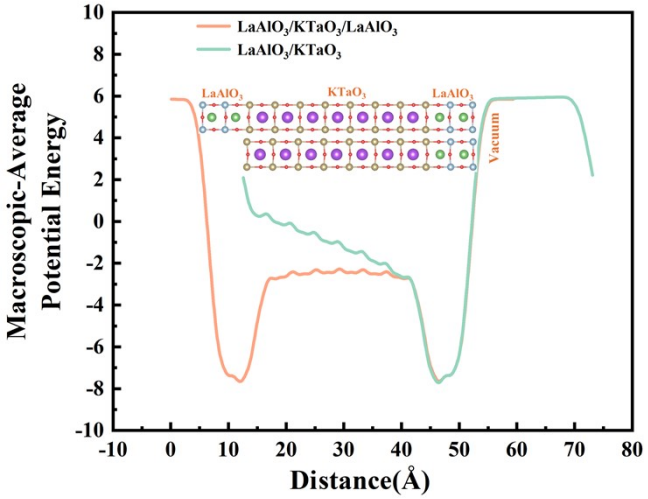

FIG. S1 The macroscopically averaged potentials are plotted along the [001] direction of the *n*-type interface $(LaAlO_3)_2/(KTaO_3)_8$ and $(LaAlO_3)_2/(KTaO_3)_{7.5}/(LaAlO_3)_2$ heterostructure.

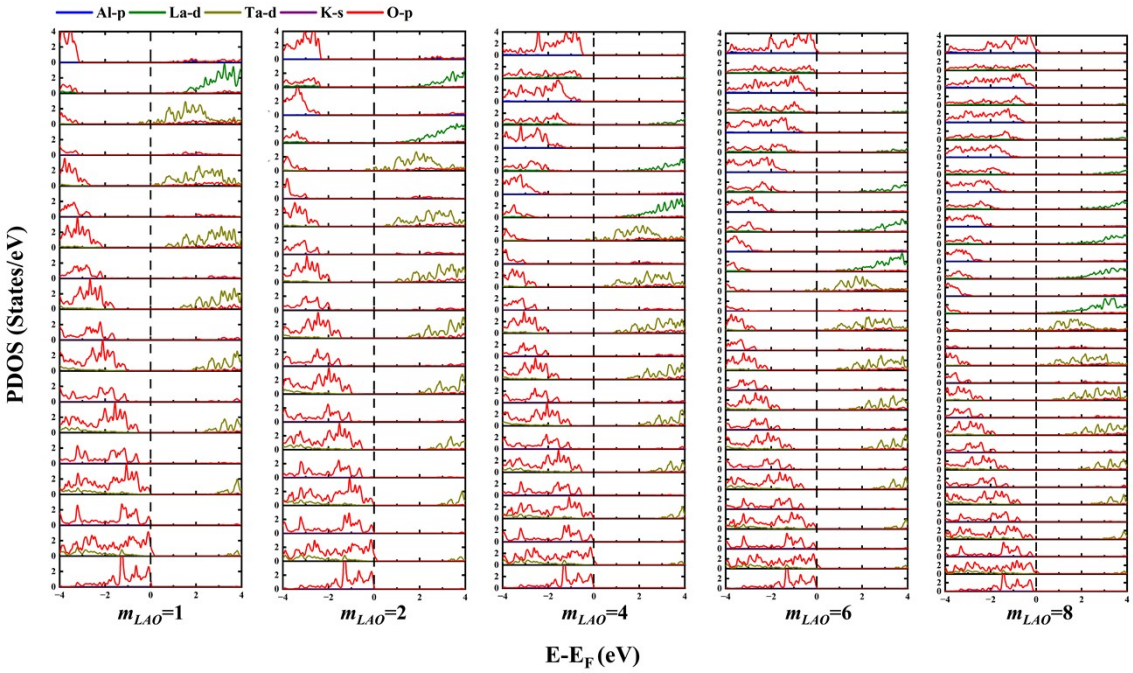

FIG. S2 Calculated layer-resolved PDOS for the *n*-type LaO^+/TaO_2^+ interfaces of $(LaAlO_3)_m/(KTaO_3)_8$ heterostructure slab models with m=1, 2, 4, 6, 8.

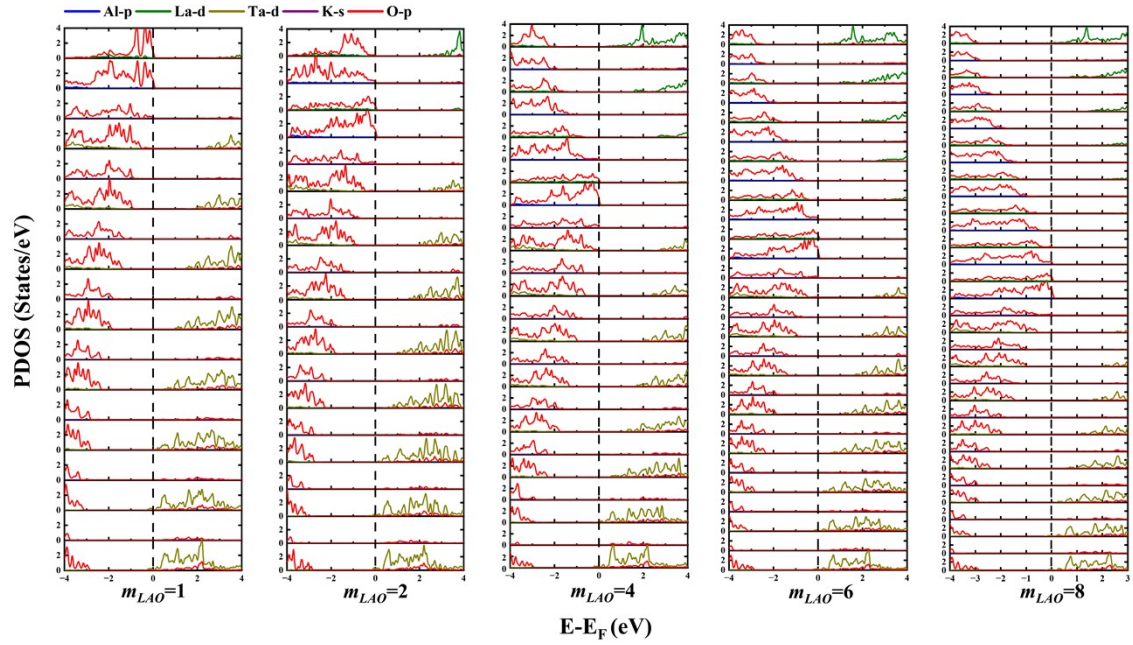

FIG. S3 Calculated layer-resolved PDOS for the *p*-type AlO_2^-/KO^- interfaces of $(LaAlO_3)_m/(KTaO_3)_8$ heterostructure slab models with m=1, 2, 4, 6, 8.

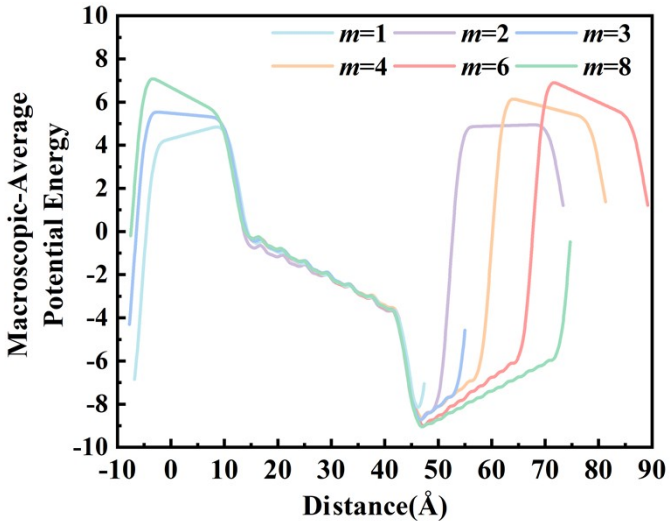

FIG. S4 The macroscopically averaged potentials are plotted along the [001] direction of the *n*-type $(LaAlO_3)_m/(KTaO_3)_8$ heterostructure slab models with m= 1, 2, 3, 4, 6, 8.

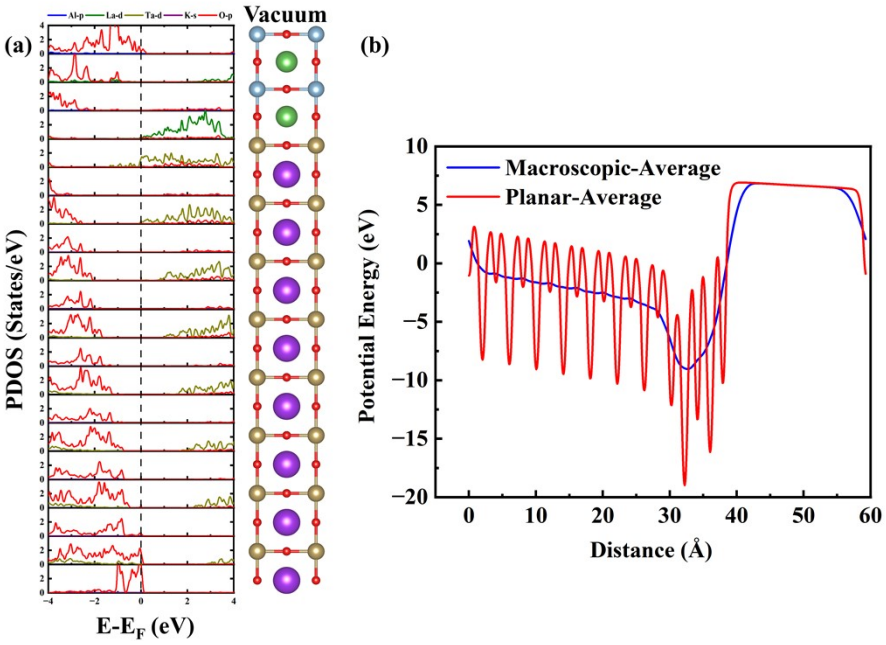

FIG. S5 (a) Calculated layer-resolved PDOS for *n*-type LaO^+/TaO_2^+ interfaces of $(LaAlO_3)_2/(KTaO_3)_8$ heterostructure slab models without structure relaxation. (b) The local electrostatic potential (red line) and macroscopically averaged potential (blue line) are plotted along the [001] direction of the heterostructure.

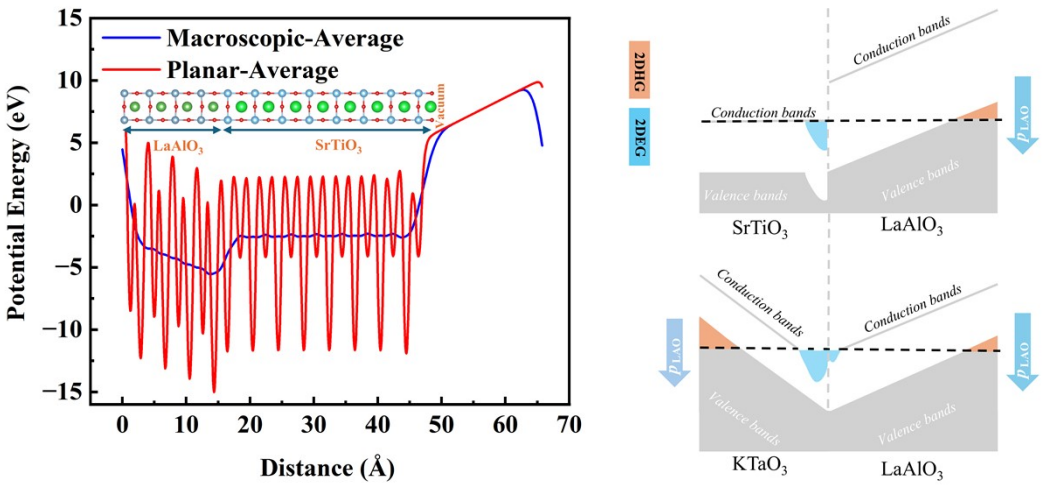

FIG. S6 The local electrostatic potential (red line) and macroscopically averaged potential (blue line) are plotted along the [001] direction of the *n*-type $(LaAlO_3)_4/(SrTiO_3)_8$ heterostructure with perfect structure relaxation. The heterostructure model is shown as inset; The schematic diagrams of band alignment in different structural models (right), where *p* stands for the initial polarization of $LaAlO_3$ or $KTaO_3$.

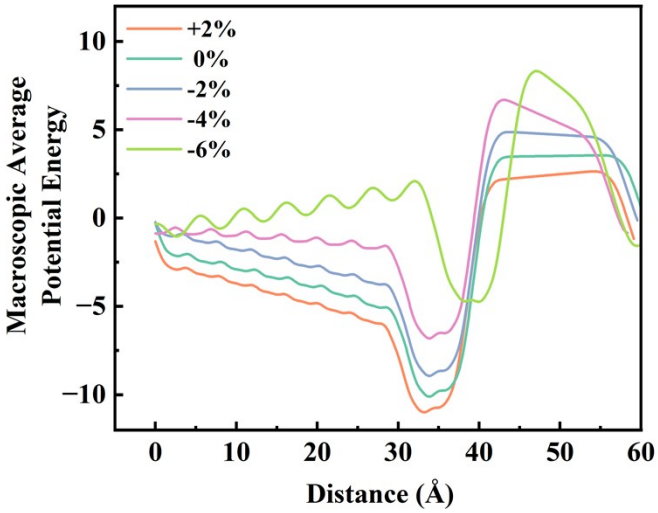

FIG. S7 The macroscopically averaged potentials are plotted along the [001] direction of the *n*-type $(LaAlO_3)_2/(KTaO_3)_8$ heterostructure with in-plane strain of 2%, 0%, -2%, -4%, -6%.

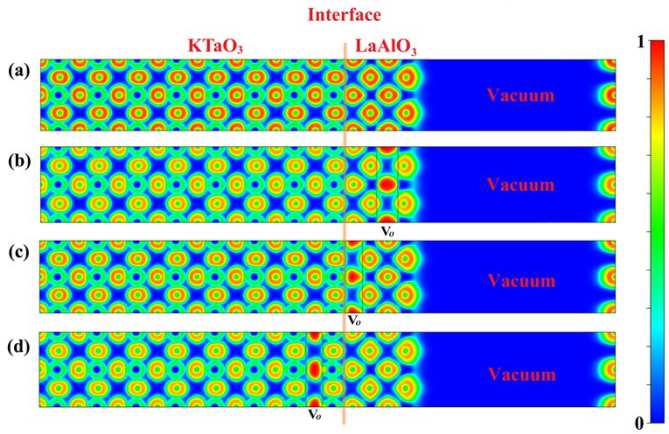

FIG. S8 The electron localization function (ELF) is plotted along the [001] direction of the *n*-type interface $(LaAlO_3)_2/(KTaO_3)_8$ heterostructure with pure (a) and O vacancy defect (b-d) located at layer 2, 4, 6.

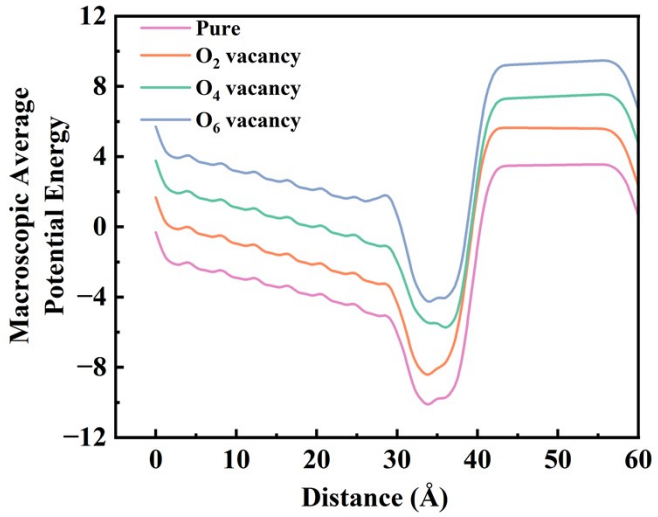

FIG. S9 The macroscopically averaged potentials are plotted along the [001] direction of the *n*-type interface $(LaAlO_3)_2/(KTaO_3)_8$ heterostructure with O vacancy defect located at layer 2, 4, 6.